

Reconstruction Performance of Blind Non Uniform Sampling in Cognitive Radio Context.

Samba TRAORE and Yves LOUET

Avenue de la Boulaie - CS 47601, F-35576, Rennes, France
{samba.traore — yves.louet}@supelec.fr

Abstract

In this paper, the authors point out the effect of noises on the non uniform periodic sampling (Multi-Coset Sampling) reconstruction performance in Cognitive Radio context. This feature is drawn by theoretical formulas regarding not only in term of Signal to Noise Ratio (SNR), but also in term of Carrier to Noise Ratio (CNR). We will show by simulation the influence of these different noises in term of Bit Error Rate (BER) and Root Mean Square Error (RMSE).

1. Introduction

New wireless applications place high demands on the quality of radio resources such as bandwidth and spectrum. Moreover, the current trends in wireless technology have increased the complexity of the receiver, more specifically its Analog to Digital Converter (ADC), due to the nature of broadband signals generated by certain applications, including communications in ultra wideband. Sampling a wideband signal at Nyquist rate (f_{nyq}) will require an ADC which consumes a lot of energy. To reduce the sampling rate, and in turn the energy consumption, several researchers have studied the possibility of Sub-Nyquist sampling. In [1]–[4], Sub-Nyquist sampling are proposed for sparse multi-band signals. This sampling technique shows that perfect reconstruction is possible when the band locations are known. Over the recent years Multi-Coset (MC) sampling has gained fair popularity and several methods of implementing sampling have been proposed [5]–[7]. The most famous architecture is composed of several parallel branches, each with a time shift followed by a uniform sampler operating at a sampling rate lower than the Nyquist rate.

In [8], we proposed a non-uniform periodic sampling scheme based on MC sampling. Our scheme detects the spectral location of the active bands in the all band sampled to reduce the average sampling frequency, the number of samples collected, and consequently the power consumption of the ADC. In this paper, we will show the influence of the SNR and CNR on the RMSE and BER of the reconstructed signal, after MC sampling, considering two reconstruction techniques.

2. Background

Let $\mathcal{M}(\mathcal{B})$ be the class of continuous real-valued signals with finite energy and band-limited to a subset \mathcal{B} .

$$\mathcal{M}(\mathcal{B}) = \{x(t) \in L^2(\mathbb{R}) : \mathbf{X}(f) = 0 \forall f \notin \mathcal{B}\} \quad (1)$$

where $\mathcal{B} = [-\frac{f_{nyq}}{2}, \frac{f_{nyq}}{2}]$ and $\mathbf{X}(f) = \int_{-\infty}^{\infty} x(t)e^{-j2\pi ft} dt$, the Fourier transform of the signal $x(t)$.

Let \mathcal{F} represent the spectral support of the signal $x(t)$ defined by:

$$\mathcal{F} = \cup_{i=1}^N [a_i, b_i] \quad (2)$$

where $\mathcal{F} \subset \mathcal{B}$ and N is the number of bands in \mathcal{B} .

Assume that the spectrum $\mathbf{X}(f)$ is divided into L cells indexed from 0 to $L - 1$. If $x(t)$ is sparse in the frequency domain so that there is no energy in certain cells. We define the set of spectral indexes $\mathcal{K} = \{k_r\}_{r=1}^q$ as the set that contains the spectral indexes of the active cells (cells with energy), where $k_r \in \mathbb{L} = \{0, 1, \dots, L - 1\}$. We define also $\bar{\mathcal{K}}$ as the complement set of \mathcal{K} in \mathbb{L} .

MC Sampling is a periodic non uniform Sub-Nyquist sampling technique which samples a signal $x(t)$ at a rate lower than its associate Nyquist rate, thereby capturing only the amount of information required for an accurate

reconstruction of the signal. In short, the process of MC can be viewed as first sampling the input signal at a uniform rate with period $T = \frac{1}{f_{nyq}}$ and then selecting only p non-uniform samples from L equidistant uniform samples. The process is repeated for consecutive segments of L uniform samples such that the p selected samples have a sampling period L . The set $\mathcal{C} = \{c_i\}_{i=1}^p$ specifies the p samples that are retained in each segment of length L . It should be noted that a good choice of the sampling pattern \mathcal{C} reduces the margin of error due to spectral aliasing and sensitivity to noise in the reconstruction process [7]. Once designed, the architecture of the classical MC sampler cannot be changed because of hardware limitations. This motivated us to find out an optimal system which fits with the spectrum of the input signal.

3. System Model

In [8], we presented a sampler that not only adapts to itself the changes in the input signal but is also remotely reconfigurable and is, therefore, not constrained by the inflexibility of hardwired circuitry. It is called it the Dynamic Single Branch Non-Uniform Sampler (DSB-NUS) or simply the DSB sampler (Fig.1)

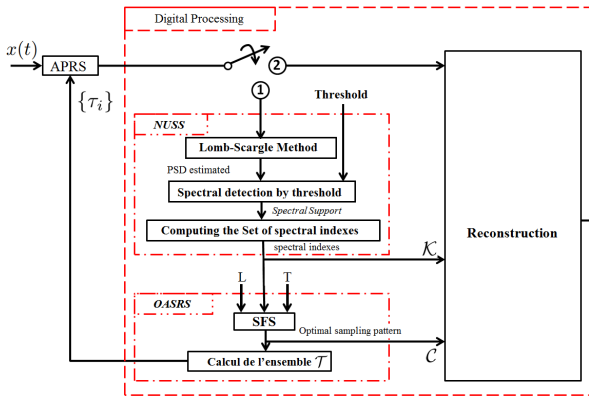


Figure 1: Dynamic Single Branch Non-Uniform Sampler

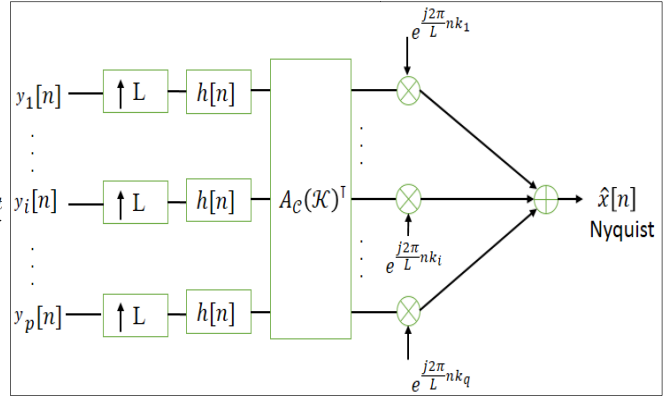


Figure 2: Recovering of $x[n]$ from non uniform samples

It operates in blind mode, without any knowledge of the input signal's spectral support and the number of bands. The DSB-NUS works in two phases: Adaptive phase and Reconstruction Phase. In Adaptation phase, when the switch is in position 1, the system has no information about $x(t)$ (number of bands N , bands location, set \mathcal{K} of spectral indexes, etc). It performs a spectral analysis on the block NUSS (Non Uniform Spectrum Sensing, estimate the Spectral support \mathcal{F} and \mathcal{K} , using Lomb-Scargle). In the Optimal Average Sampling Rate Search block (OASRS), according to (L, T, \mathcal{K}) , used the Sequential Forward Selection (SFS) algorithm to find the optimal sampling pattern \mathcal{C} and then the optimal set of sampling instants $\{\tau_i\}$. In the Reconstruction phase, when the switch is in position 2, the DSB-NUS sampler performs MC reconstruction.

Next, we will study the influence of the SNR and CNR on the Root Mean Square Error of the reconstructed signal, after MC sampling, follow two reconstruction techniques.

4. Reconstruction

We express the non uniform samples $x(t_n)$ at the output of the Non Uniform sampler (NUS) block in terms of periodic sequences $y_{ci}[n]$, where $c_i \in \mathcal{C}$ specifies the position of the sample from consecutive segments of L uniform samples. The Fourier transform, $Y_i(f)$, of the sampled sequence $y_{ci}[n]$, is related the Fourier transform, $X(f)$, of the unknown signal $x(t)$ by the following equation :

$$\exp(-j2\pi f c_i T) Y_i(f) = \frac{1}{LT} \sum_{k=-\frac{L}{2}-1}^{\frac{L}{2}-1} \exp\left(j2\frac{\pi k c_i}{L}\right) X\left(f + \frac{k}{LT}\right) \quad (3)$$

where, $0 \leq i \leq p-1$, and $f \in \mathcal{B}_0 = [0, \frac{1}{LT}]$. Note that $X(f) = 0$ for $f \notin \mathcal{B} = [-\frac{f_{nyq}}{2}, \frac{f_{nyq}}{2}]$. The expression in (3) can be written in its matrix form :

$$\mathbf{y}(f) = \mathbf{A}_e(\mathcal{K})\mathbf{z}(f) + \mathbf{A}_e(\mathcal{K})\mathbf{b}_1(f) + \mathbf{A}_e(\bar{\mathcal{K}})\mathbf{b}_2(f) \quad (4)$$

where, $f \in \mathcal{B}_0$ and $\mathbf{y}(f)$ is a vector of size $p \times 1$ whose i^{th} element is given by:

$$y_i(f) = \exp(-j2\pi f c_i T) Y_i(f) \quad (5)$$

$\mathbf{A}_e(\mathcal{K})$ is a matrix of size $p \times p$ whose $(i, l)^{th}$ element is given by:

$$[\mathbf{A}_e(\mathcal{K})]_{il} = \frac{1}{LT} \exp\left(j2\frac{\pi k_l c_i}{L}\right), \text{ where } k_l \in \mathcal{K} \text{ and } c_i \in \mathcal{C} \quad (6)$$

$\mathbf{A}_e(\overline{\mathcal{K}})$ is a matrix of size $p \times L - p$ whose $(i, l)^{th}$ element is given by:

$$[\mathbf{A}_e(\overline{\mathcal{K}})]_{il} = \frac{1}{LT} \exp\left(j2\frac{\pi k_l c_i}{L}\right), \text{ Where } k_l \in \overline{\mathcal{K}} \text{ and } c_i \in \mathcal{C} \quad (7)$$

$\mathbf{b}_1(f)$ is a vector of size $p \times 1$ whose elements represent the noise in the active cells indexes by \mathcal{K} .

$\mathbf{b}_2(f)$ is a vector of size $L - p \times 1$ whose elements represent the noise in the non active cells indexes by $\overline{\mathcal{K}}$.

$\mathbf{z}(f)$ represents the unknown vector of size $p \times 1$ whose l^{th} element is given by:

$$z_l(f) = X\left(f + \frac{k_l}{LT}\right), \text{ where } k_l \in \mathcal{K} \quad (8)$$

The reconstruction of $x(t)$, requires to solve the linear equation (4). If $\mathbf{A}_e(\mathcal{K})$ is full column rank matrix, the unique solution of (4) is given by:

$$\mathbf{z}(f) = (\mathbf{A}_e(\mathcal{K}))^{-1} \mathbf{y}(f) + \mathbf{b}_1(f) + (\mathbf{A}_e(\mathcal{K}))^{-1} \mathbf{A}_e(\overline{\mathcal{K}}) \mathbf{b}_2(f) \quad (9)$$

There are two ways to reconstruct $x(t)$. For the first method, once $\mathbf{z}(f)$ is found, the inverse Fourier transform achieves the time domain representation of each cell, $x_r(t)$ Fourier transform of $X\left(f + \frac{r}{LT}\right)$. The reconstructed signal in time domain is written as

$$x(t) = \sum_{r=0}^{p-1} x_r(t) \exp\left(j\frac{2\pi r t}{LT}\right) \quad (10)$$

The second method regards a simple time domain solution. At first the sequence $y_{ci}[n]$ is upsampled with L and filtered. The interpolation filter is defined by $h[n] = h_r \exp\left(\frac{j\pi n}{L}\right)$ with cut off frequencies at $f_c = \frac{1}{LT}$. After filtering a linear combination is done by using $(\mathbf{A}_e(\mathcal{K}))^{-1}$ (see Fig.2). Then, the reconstruction formula is:

$$x(nT) = \sum_{i=0}^p \sum_{l=0}^p [\mathbf{A}_e(\mathcal{K})]_{il} (h[n] * y_{ci}[n]) \exp\left(j\frac{2\pi k_l n}{L}\right) \quad (11)$$

To compare the performance of the reconstruction method we use the Root Mean Square Error value, define as:

$$RMSE = \frac{\|x[n] - \hat{x}[n]\|_2}{\|x[n]\|_2} \quad (12)$$

where $x[n]$ is the Nyquist Samples and $\hat{x}[n]$ the reconstructed Nyquist samples from MC Samples.

5. Numerical results

For simulations, we consider a modulated 4-QAM signal with a rolloff equal to 0.5, symbol rate equal to 1×10^6 symbols/second. The frequency carrier is unknown and the wideband of interest is in the range $[-20, 20]$ MHz. The signal is corrupted by the additive white Gaussian noise on the actives cells with a certain SNR (the power ratio between the signal and the noise in the actives cells) and a certain CNR (the power ratio between the signal in the actives cells and the noise in the complement of actives cells). For the MC Sampling we take $L = 128$, for the filter h_r we used the MATLAB function $h_r = \text{fir1}(Nh, \frac{1}{L})$, with $Nh = 4 \times L - 1$.

In the Fig.3, we can show that for CNR = 100 dB and 50 dB the BER curve of both of the two reconstruction method are quite equal to the theory curve. But after CNR = 20 dB, both curves diverge from the theoretical curve for a high E_b/N_0 . It should be noted that, E_b/N_0 is calculated as a function of SNR.

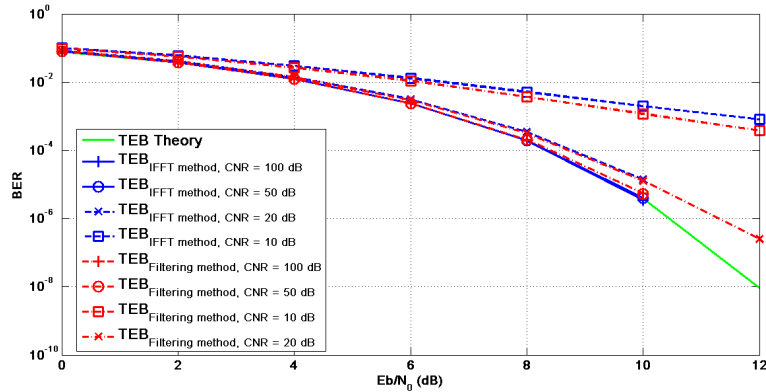


Figure 3: Error Rate versus E_b/N_0 , for different value of CNR

In the Fig.4, we can observe that for $\text{CNR} = 100 \text{ dB}$ and 60 dB the RMSE for Filtering method tends to a limit value for all SNR higher than 50 dB , while the RMSE for IFFT method begins to move towards a limit value for SNR greater than the root of the CNR inverse. For $\text{CNR} = 20 \text{ dB}$ of both of the two reconstruction method are quite equal to the root of the CNR inverse for high SNR.

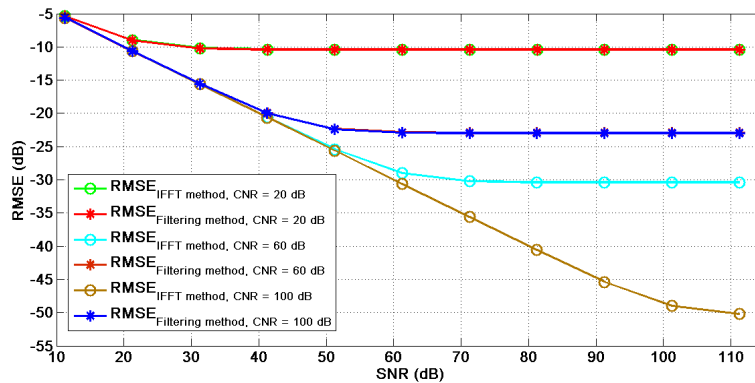


Figure 4: RMSE versus SNR, for different value of CNR

5. Conclusion

In this paper, we have shown by simulation the influence of Signal to Noise Ratio and Carrier to Noise Ratio on the Multi-Coset Sampling Reconstruction in term of Bit Error Rate and Root Mean Square Error. After observation we can say that The Root Mean Square Error and the Bit Error Rate are very sensitive not only to the variation of the Signal to Noise Ratio for high Carrier to Noise Ratio but also to the variation of the Carrier to Noise Ratio for high Signal to Noise Ratio. Authors' perspectives are find out the exact relation between the Bit Error Rate, Root Mean Square Error, Signal to Noise Ratio and the Carrier to Noise Ratio.

6. References

- [1] M. Mishali et Y. C. Eldar, « From theory to practice: Sub-Nyquist sampling of sparse wideband analog signals », *Sel. Top. Signal Process. IEEE J. Of*, vol. 4, n° 2, p. 375-391, 2010.
- [2] S. Kirolos, J. Laska, M. Wakin, M. Duarte, D. Baron, T. Ragheb, Y. Massoud, et R. Baraniuk, « Analog-to-information conversion via random demodulation », in *Design, Applications, Integration and Software, 2006 IEEE Dallas/CAS Workshop on*, 2006, p. 71-74.
- [3] J. Laska, S. Kirolos, Y. Massoud, R. Baraniuk, A. Gilbert, M. Iwen, et M. Strauss, « Random sampling for analog-to-information conversion of wideband signals », in *Design, Applications, Integration and Software, 2006 IEEE Dallas/CAS Workshop on*, 2006, p. 119-122.
- [4] R. S. Prendergast, B. C. Levy, et P. J. Hurst, « Reconstruction of band-limited periodic nonuniformly sampled signals through multirate filter banks », *Circuits Syst. Regul. Pap. IEEE Trans. On*, vol. 51, n° 8, p. 1612-1622, 2004.
- [5] M. E. Dominguez-Jiménez et N. González-Prelcic, « Analysis and design of multirate synchronous sampling schemes for sparse multiband signals », 2012.
- [6] T. Moon, N. Tzou, X. Wang, H. Choi, et A. Chatterjee, « Low-cost high-speed pseudo-random bit sequence characterization using nonuniform periodic sampling in the presence of noise », in *VLSI Test Symposium (VTS), 2012 IEEE 30th*, 2012, p. 146 -151.
- [7] R. Venkataramani et Y. Bresler, « Optimal sub-Nyquist nonuniform sampling and reconstruction for multiband signals », *Signal Process. IEEE Trans. On*, vol. 49, n° 10, p. 2301-2313, 2001.
- [8] S. Traoré, B. Aziz, et D. Le Guennec, « Dynamic Single Branch Non-Uniform Sampler », presented in DSP 2013, International Conference on Digital Signal Processing, Santorini, Greece, 2013.